applied sciences

MDPI

Article

Histological Bone-Healing Evaluation of Critical-Size Defects Filled with β-Tricalcium Phosphate in Rat Tibiae

Ana Maria Veiga Vasques [1], Carlos Roberto Emerenciano Bueno [1], Maria Rosa Felix de Souza Gomide Guimarães [2], Diego Valentim [1], Ana Cláudia Rodrigues da Silva [1], Francine Benetti [3], João Miguel Marques Santos [4,*], Luciano Tavares Angelo Cintra [1] and Eloi Dezan Junior [1]

[1] Endodontic Section, Department of Preventive and Restorative Dentistry, School of Dentistry, São Paulo State University (UNESP), Araçatuba 16015-050, SP, Brazil; anavvasques@hotmail.com (A.M.V.V.); c.bueno@unesp.br (C.R.E.B.); dvalentim_5@hotmail.com (D.V.); claudia.silva@unesp.br (A.C.R.d.S.); luciano.cintra@unesp.br (L.T.A.C.)
[2] Endodontic Section, Department of Dentistry, School of Dentistry, University Center São Lucas, Porto Velho 76805-846, RO, Brazil
[3] Endodontic Section, Department of Restorative Dentistry, Faculty of Dentistry, Federal University of Minas Gerais (UFMG), Belo Horizonte 31270-901, MG, Brazil
[4] Institute of Endodontics, Faculty of Medicine, University Coimbra, 3004-531 Coimbra, Portugal
* Correspondence: jsantos@fmed.uc.pt; Tel.: +351-239-249-151

Abstract: Bone defects may be a result of different pathologies and represent a challenge in different fields of dentistry. Techniques for the correction of bone defects involving the use of several types of grafts have been proposed. This study evaluated bone repair in rat tibiae after surgically created critical-size defects were filled with β-tricalcium phosphate (RTR®, Septodont, FR). Critical-size bone defects were created in the tibiae of 32 male Wistar rats, which were divided into four groups (n = 8): Control 30 days, Control 90 days, RTR® 30 days, and RTR® 90 days. After the experimental period, the animals were euthanized and specimens were collected, embedded in paraffin, serially cut, and stained with hematoxylin and eosin to evaluate the inflammatory and repair response. Two parameters were analyzed: neoformed bone tissue areas (NBA) and neoformed cortical areas (NCA). Statistical analysis was performed by ANOVA and Tukey's test ($p < 0.05$). The RTR® group demonstrated superior bone healing compared with the control group in both analyzed parameters (NBA and NCA), with repair of the cortical bone and bone-tissue formation in the central region of the defect, which showed partial repair in the defect area ($p < 0.05$). RTR® enhanced bone neoformation in the adopted experimental model and may be a useful biomaterial to boost healing in cases of critical-size bone defects.

Keywords: β-tricalcium phosphate; bone regeneration; bone substitute; RTR®

Citation: Vasques, A.M.V.; Bueno, C.R.E.; Guimarães, M.R.F.d.S.G.; Valentim, D.; da Silva, A.C.R.; Benetti, F.; Santos, J.M.M.; Cintra, L.T.A.; Dezan Junior, E. Histological Bone-Healing Evaluation of Critical-Size Defects Filled with β-Tricalcium Phosphate in Rat Tibiae. *Appl. Sci.* **2024**, *14*, 3821. https://doi.org/10.3390/app14093821

Academic Editor: Dorina Lauritano

Received: 1 March 2024
Revised: 5 April 2024
Accepted: 28 April 2024
Published: 30 April 2024

1. Introduction

Bone defects arising from dental extractions, trauma, or pathology present significant challenges in surgical rehabilitation due to the physiological resorption of bone, which often leaves insufficient healthy tissue for effective repair [1–4]. Autogenous bone grafting utilizing the patient's own bone tissue is traditionally considered the gold standard for repairing such defects. This preference is due to the graft's complete compatibility with the recipient site, which results in notable osteogenesis, osteoconductivity, and osteoinductivity [5]. Despite its advantages, autogenous bone grafting is limited by the available volume of bone and the potential for donor-site morbidity, prompting the search for alternative bone substitutes [6].

The search for viable alternatives has led to the exploration of biomaterials, both natural and synthetic, designed to mimic the function of human tissues and organs without the need for donor tissue [7]. The effectiveness of these graft materials in dental applications is measured by their ability to support bone regeneration by acting as scaffolds for

bone growth. These materials are evaluated for osteogenesis (the introduction of bone-forming cells), osteoconductivity (the support of cell proliferation), and osteoinductivity (the induction of cell differentiation into osteoblasts), with the ideal material exhibiting all three properties. However, while autogenous grafts meet these standards, biomaterials tend to exhibit strong osteoconductivity but fall short in osteogenic and osteoinductive capabilities [5,8].

Bone substitutes are divided according to source and immune response into four categories: autogenous (obtained from the patient), homogenous (bone graft from a bone bank), heterogenous (graft from a different species), and alloplastics (produced and synthesized in the laboratory). β-tricalcium phosphate (β-TCP) is an example of an alloplastic ceramic material that has demonstrated good biocompatibility, and several studies have demonstrated its ability to stimulate bone formation by osteoconduction in the repair of bone defects [9–16].

RTR® (Septodont, Saint-Maur-des-Fosses, France) is a bone substitute comprising β-TCP granules of different sizes, ranging from 500 µm to 1 mm, that is used for bone-defect reconstruction in surgical procedures in dentistry [17], with satisfactory clinical and radiographic results for bone neoformation [17–20]. RTR® has been shown to positively influence the differentiation of osteoblasts, the expression of bone morphogenetic proteins (BMPs), and the subsequent expression of markers critical for bone formation, such as alkaline phosphatase, type I collagen, osteopontin, and osteocalcin [18,19].

The animal model adopted in this study was proposed by Bernabé et al. [20]. Different sites are used to evaluate new bone formation in rats, such as the calvaria, tibia and mandible. The rat tibia was chosen because it was possible to keep the materials in contact with the bone tissue, thus representing a condition similar to that in which bone grafts are normally used in humans. The significance of the bone-defect size was also considered, emphasizing defects of a critical size—those that would not naturally repair over the animal's lifespan—as per Schmitz & Hollinger [21].

Addressing the paucity of research on the capabilities of RTR® for inducing bone neoformation in animal models, this study aims to assess its effectiveness in repairing critical surgical bone defects by examining the integrity and quality of the newly formed bone tissue. The null hypothesis posits that RTR® lacks the ability to stimulate bone neoformation in rat tibias.

2. Materials and Methods

2.1. Experimental Models

This study was approved by the Committee on Ethical Conduct in the Use of Animals in Experimentation (No.: 00249-2016). In total, 32 male rats (*Rattus albinus*, Wistar) weighing 450 to 500 g were used. The animals were housed in a controlled-temperature environment (22 °C ± 1 °C) with a 12 h light cycle and access to food and water ad libitum. The animals were randomly assigned to one of four experimental groups (n = 8): Control 30 days, Control 90 days, RTR® 30 days, and RTR® 90 days.

2.2. Surgical Procedures

The animals were first anesthetized intramuscularly with a mixture of ketamine 75 mg/kg (Cetamin 10%, Syntec, São Paulo, Brazil) and xylazine 25 mg/kg (Xilazin 2%, Syntec, São Paulo, Brazil). After trichotomy and antisepsis of the surgical site, a linear incision of about 15 mm was made over the tibia, involving the skin, muscle, and periosteum of the animal to expose the bone tissue (Figure 1). Bone defects were created with a 4.1-mm diameter trephine drill (3i Implant Innovations Inc., Palm Beach Gardens, FL, USA) in the tibia of each animal [20]. Then, two marks were made on the ends of the bone defects using a small cavity filled with an amalgam to assist in our identification of the bone defects during analysis (Figure 2). Bone defects were treated according to the conditions set for each group. In the Control Group, bone defects were filled only with blood clots, and in the RTR Group, the defects were filled with RTR® (Septodont, Saint-Maur-des-Fossés, France).

After the bone defects were filled, the tissues were carefully repositioned and sutured with 5.0 and 4.0 silk thread (Ethicon, São Paulo, Brazil).

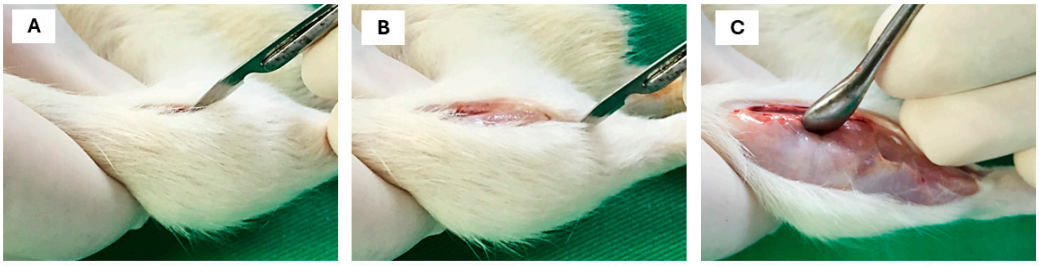

Figure 1. (**A**) linear incision; (**B**) a 15 mm incision was made over the tibia, involving the skin, muscle and periosteum; (**C**) divulsion of tissues to expose the tibia.

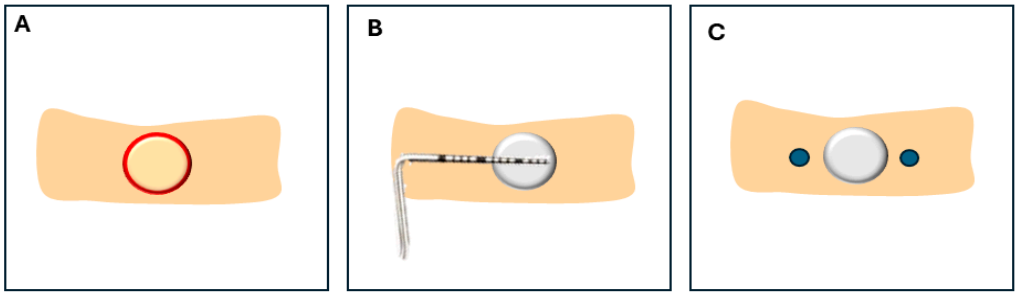

Figure 2. Representative diagram of the bone defect. (**A**) Bone defects were created with a 4.1-mm diameter trephine drill; (**B**) checking the diameter of the bone defect with a millimeter periodontal probe; (**C**) two marks were created on the ends of the bone defects using a small cavity filled with an amalgam to assist our identification of the bone defects during analysis.

2.3. Sample Collection

After the 30- and 90-day experimental periods, the animals were euthanized with an overdose of anesthetic solution. Their tibias were removed and stored in a 10% formaldehyde solution for 24 h and decalcified in 10% buffered EDTA (Sigma-Aldrich, Darmstadt, Germany), which was changed once a week for three months. The samples were embedded in paraffin after conventional laboratory processing. Then, 6-µm-thick semi-serial sections were cut and stained with hematoxylin and eosin for analysis under an optical microscope (DM 4000B, Leica, Wetzlar, Germany).

2.4. Histomorphometric Analysis

Histological analysis was used to describe the bone-repair process in each surgical defect created in ruptured cortical bones and the characteristics of the new tissue occupying this region. Overall, six histological sections of the central area of the surgical defect of each specimen were chosen. Each section was imaged, and the images were transferred to ImageLab 2000 (Diracom Bio Informática LTDA, Vargem Grande do Sul, São Paulo, Brazil).

In each image, the area to be analyzed (corresponding to the region of the tibia in which the bone defect had been created) was delimitated and called the total area (TA). Neoformed bone area (NBA) areas were selected and delimited within the total area (TA). The TA value was considered to be 100% of the analyzed area, and the NBA value was calculated as a percentage of TA as follows: NBA% = 100 × NBA/TA (mm^2) [20].

To measure the cortical bone, the total analyzed cortical area (TCA) was considered to be 100%. For TCA, neoformed cortical areas (NCA) were identified and delimited as follows: NCA% = 100 × NCA/TCA (mm^2) [20].

2.5. Statistical Analyses

The values were tabulated for each experimental group, and the data were analyzed using Sigma Plot (V12.0 Systat Software Inc., San Jose, CA, USA). After the Shapiro–Wilk test of normality, analysis of variance (ANOVA) was performed, followed by Tukey's post-test with a significance level of $p < 0.050$.

3. Results

3.1. Control 30 Days

All specimens showed minimum neoformed bone area (NBA), with an average percentage of 2.46%. After the same period of 30 days, the RTR group presented an average NBA percentage of 31.31%, for a statistically significant difference between the groups ($p < 0.05$). Differentiating connective tissue with a small number of fibroblasts occupied the surgical defects, which showed no neoformation of the ruptured cortical bone (Figure 3A) (Table 1).

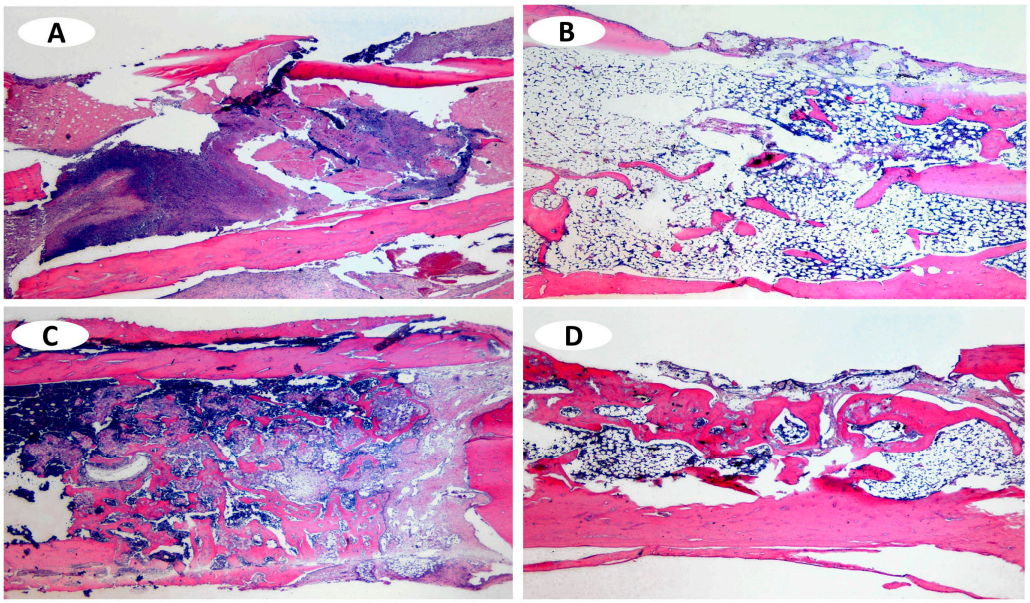

Figure 3. (**A**) Control 30 days: minimum bone repair; (**B**) RTR® 30 days: cortical neoformation was complete with inflammatory infiltrate; (**C**) Control 90 days: partial repair of the cortical bone; (**D**) RTR® 90 days: bone cortical repair with a thinner neoformed tissue.

Table 1. Mean percentage and standard deviation of total newly neoformed bone area (NBA) and newly neoformed cortical areas (NCA) in the control and RTR groups at 30 and 90 days.

Groups		30 Days		90 Days	
		Mean (%)	SD	Mean (%)	SD
Control	NBA	2.46 ^{A}	±0.43	15.10 ^{A}	±1.83
	NCA	0.09 ^{a}	±0.09	22.01 ^{a}	±2.75
RTR®	NBA	31.31 ^{B}	±3.88	36.80 ^{B}	±5.87
	NCA	34.95 ^{b}	±5.01	42.84 ^{b}	±5.50

Different superscript letters represent statistically significant differences $p < 0.05$. Comparisons: capital letters (Control vs. RTR in NBA); lowercase (Control vs. RTR in NCA).

3.2. Control 90 Days

In this group, we observed partial repair of the NCA and the NBA. Compared to the Control 30 days group, more areas isolated of immature bone-tissue formation were observed close to the fibrous connective tissue in the area of the surgical defect. In the

cortical area, the repair was more extensive, with an area 22.01% greater compared to that in the 30 days group (Figure 3C) (Table 1).

3.3. RTR® 30 Days

The cortical neoformation NCA was complete, with an average area percentage of 34.95%. It is possible to observe an inflammatory infiltrate and the total closure of the bone defect, with thinner tissue than the original tibial bone. Also, small formations of neoformed bone area (NBA) in the central region of the defect were found, but there were no RTR® particle remnants (Figure 3B) (Table 1).

3.4. RTR® 90 Days

After 90 days, cortical bone repair (NCA) was complete, with an average percentage of 42.84%. Newly formed tissue thinner than the original tibial bone and formations of immature bone tissue in the region of the surgical defect were observed (NBA) (Figure 3D and Table 1), with no remnants of RTR® particles.

4. Discussion

The histological and histometric analysis of the effect of RTR® (β-TCP) on the bone-repair process in surgically induced bone defects in rat tibiae revealed that RTR® promotes bone neoformation. This finding aligns with those of prior studies on β-TCP formulations, which have been noted for their biocompatibility, biodegradation [9,22–25], and osteoconductive capacities [10,22,26–29]. The findings of Bueno et al. [30] and Truedsson et al. [31], highlighting the influence of the physical and chemical properties of β-TCP granules, such as shape, size, and porosity, on osteoblastic behavior, lend further credence to the theory that these characteristics are crucial for enhancing bone regeneration [32,33]. Additionally, research by Benetti et al. [34] that investigated the inflammatory response and biomineralization induced by RTR® in subcutaneous tissues underscores its biocompatibility and potential to promote bone mineral formation.

Martinez et al. [33] have suggested that bone neoformation is intricately linked to the degradation of β-TCP particles, which ostensibly enhances osteoblastic activities. Our observations of diminished inflammatory responses and reduced graft-particle presence after 90 days, attributable to osteoclastic activity and subsequent bone neoformation in intimate contact with the biomaterial, align with these insights.

To better evaluate the development and formation of calcifications in hard tissue, researchers can also use an alkaline phosphatase (ALP) marker, as its enzymatic activity is related to bone cell development [35,36]. A study by Fathima & Harish [36], which compared morphological changes and ALP levels in fibroblasts cultured with various commercially available graft materials, revealed that RTR® induced significant morphological alterations and elevated ALP activity, signifying its superior bone-regeneration capacity.

Further research examining the effectiveness of bone grafts in patients with chronic periodontitis through a comparison of RTR®-associated platelet-rich fibrin (PRF) and a β-TCP allograft in treating class II mandibular furcation defects concluded that both materials substantially improved tissue regeneration [37]. This finding underscores the importance of carefully selecting experimental models that closely mimic human conditions and exhibit minimal variability [38], considering factors like gender and age [31,39]. The experimental model we adopted, rat tibiae [40–42], has good reproducibility and some similarities to human bone tissue, as tibiae are long bones with straight cortices but no contour and a medullary canal with great potential for differentiating osteoblasts and formation of bone tissue [41].

In our study, critical bone defects measuring 4.1 mm in diameter were strategically selected based on findings by Ribeiro et al. [42] and Mendes et al. [43], which suggested that defects of 3 mm diameter in rat tibias can heal spontaneously and might not accurately represent the challenges posed by larger defects. The absence of bone repair in the

30-day clot group with these larger defects confirms the critical nature of larger defects for regeneration, aligning with similar observations by Bernabé et al. [20].

Periods below 30 days make it impossible to observe the complete healing of defects, even with smaller cavities. Borrasca et al. [41] found similar results, as the 2 mm diameter bone defects in rat tibiae showed only a thin fibrous capsule containing collagen fibers, fibroblasts, a small number of blood vessels, a small number of inflammatory cells and immature bone trabeculae in their 10-day clot group.

The 90-day clot group showed partial repair of the cortical bone and small isolated formations of immature bone tissue in the surgical defect area. Bernabé et al. [20] found similar results for the same period, as they found no neoformed bone in critical defects. Cunha et al. [44] observed repair of the longitudinal fissures in rat tibiae with immature bone tissue in their 45-day clot group.

The RTR® group, after 30 and 90 days, showed better repair of the cortical bone and more bone tissue inside the defect than the clot group. Similar findings have been observed in rat calvary injuries [45] after 45 and 60 days [25].

Martinez et al. [33] found that β-TCP showed great bone-formation capacity, observing osteoblasts and osteocytes in close contact with the RTR® biomaterial after 30 days. Hirota et al. [19] also found bone repair. Despite evaluating critical bone defects, they found that RTR® created an effective substitute associated with autogenous bone in rat jaws after seven days. Another study evaluated critical defects in the jaws of dogs for 30 days, finding that RTR® enhanced neoformation of bone [45].

In defects surgically created after the extraction of rat molars [3], the authors found intense inflammatory process after five days and bone formation after 20 days following association of β-TCP with mesenchymal cells. These studies show the osteoinductive capacity of β-TCP, corroborating our findings.

5. Conclusions

Our investigation into the use of RTR® (β-TCP) as a bone substitute in critical-sized bone defects demonstrates its capacity to favor bone neoformation within our experimental model, positioning RTR® as a viable option for the treatment of critically sized bone cavities.

Author Contributions: Conceptualization, A.M.V.V., C.R.E.B., A.C.R.d.S., F.B., L.T.A.C. and E.D.J.; Data curation, A.M.V.V., M.R.F.d.S.G.G., D.V., A.C.R.d.S., F.B. and J.M.M.S.; Formal analysis, A.M.V.V., C.R.E.B., M.R.F.d.S.G.G., A.C.R.d.S., F.B. and J.M.M.S.; Funding acquisition, J.M.M.S., L.T.A.C. and E.D.J.; Investigation, C.R.E.B., D.V., L.T.A.C. and E.D.J.; Methodology, E.D.J.; Project administration, L.T.A.C. and E.D.J.; Resources, L.T.A.C. and E.D.J.; Supervision, L.T.A.C. and E.D.J.; Validation, J.M.M.S. and E.D.J.; Writing—original draft, A.M.V.V.; Writing—review & editing, A.M.V.V., C.R.E.B., M.R.F.d.S.G.G., D.V., A.C.R.d.S., F.B., J.M.M.S., L.T.A.C. and E.D.J. All authors have read and agreed to the published version of the manuscript.

Funding: This research received no external funding.

Institutional Review Board Statement: The animal study protocol was approved by the Committee on Ethical Conduct in the Use of Animals in Experimentation School of Dentistry (No.: 00249-2016).

Informed Consent Statement: Not applicable.

Data Availability Statement: The original contributions presented in the study are included in the article, further inquiries can be directed to the corresponding author.

Conflicts of Interest: The authors declare no conflicts of interest.

References

1. Zerbo, I.R.; Zijderveld, S.A.; de Boer, A.; Bronckers, A.L.; de Lange, G.; ten Bruggenkate, C.M.; Burger, E.H. Histomorphometry of human sinus floor augmentation using a porous beta-tricalcium phosphate: A prospective study. *Clin. Oral. Implant. Res.* **2004**, *15*, 724–732. [CrossRef] [PubMed]
2. Wu, W.; Chen, X.; Mao, T.; Chen, F.; Feng, X. Bone marrow-derived osteoblasts seeded into porous beta-tricalcium phosphate to repair segmental defect in canine's mandibula. *Ulus Travma Acil Cerrahi Derg* **2006**, *12*, 268–276. [PubMed]

3. Sava-Rosianu, R.; Podariu, A.C.; Popovici, R.A.; Tanasie, G.; Iliuta, L.; Oancea, R. Alveolar bone repair using mesenchymal stem cells placed on granular scaffolds in a rat model. *Dig. J. Nanomater. Biostructures DJNB* **2013**, *8*, 303–311.
4. Sarnadas, M.; Marques, J.A.; Baptista, I.P.; Santos, J.M. Impact of Periodontal Attachment Loss on the Outcome of Endodontic Microsurgery: A Systematic Review and Meta-Analysis. *Medicina* **2021**, *57*, 922. [CrossRef] [PubMed]
5. Mazzoneto, R.; Netto, H.D.; Nascimento, F.F. Biomateriais: Conceitos e aplicações. In *Enxertos ósseos em Implantodontia*, 1st ed.; Napoleão Quitessence: Nova Odessa, Brazil; Volume 1, pp. 78–104, ISBN 9788560842322.
6. Nassr, A.; Khan, M.H.; Ali, M.H.; Espiritu, M.T.; Hanks, S.E.; Lee, J.Y.; Donaldson, W.F.; Kang, J.D. Donor-site complications of autogenous nonvascularized fibula strut graft harvest for anterior cervical corpectomy and fusion surgery: Experience with 163 consecutive cases. *Spine J.* **2009**, *9*, 893–898. [CrossRef] [PubMed]
7. Szabó, G.; Suba, Z.; Hrabák, K.; Barabás, J.; Németh, Z. Autogenous bone versus beta-tricalcium phosphate graft alone for bilateral sinus elevations (2- and 3-dimensional computed tomographic, histologic, and histomorphometric evaluations): Preliminary results. *Int. J. Oral. Maxillofac. Implant.* **2001**, *16*, 681–692.
8. Sequeira, D.B.; Diogo, P.; Gomes, B.P.F.A.; Peça, J.; Santos, J.M.M. Scaffolds for Dentin–Pulp Complex Regeneration. *Medicina* **2024**, *60*, 7. [CrossRef] [PubMed]
9. Damlar, I.; Erdoğan, Ö.; Tatli, U.; Arpağ, O.F.; Görmez, U.; Üstün, Y. Comparison of osteoconductive properties of three different β-tricalcium phosphate graft materials: A pilot histomorphometric study in a pig model. *J. Cranio-Maxillofac. Surg.* **2015**, *43*, 175–180. [CrossRef] [PubMed]
10. Leventis, M.D.; Fairbairn, P.; Dontas, I.; Faratzis, G.; Valavanis, K.D.; Khaldi, L.; Kostakis, G.; Eleftheriadis, E. Biological response to β-tricalcium phosphate/calcium sulfate synthetic graft material: An experimental study. *Implant Dent.* **2014**, *23*, 37–43. [CrossRef] [PubMed]
11. Herrera, D.; Lodoso-Torrecilla, I.; Ginebra, M.P.; Rappe, K.; Franch, J. Osteogenic differentiation of adipose-derived canine mesenchymal stem cells seeded in porous calcium-phosphate scaffolds. *Front. Vet. Sci.* **2023**, *10*, 1149413. [CrossRef] [PubMed]
12. Sumii, J.; Nakasa, T.; Kato, Y.; Miyaki, S.; Adachi, N. The Subchondral Bone Condition During Microfracture Affects the Repair of the Osteochondral Unit in the Cartilage Defect in the Rat Model. *Am. J. Sports Med.* **2023**, *51*, 2472–2479. [CrossRef] [PubMed]
13. Amaral, S.S.; Lima, B.S.D.S.; Avelino, S.O.M.; Spirandeli, B.R.; Campos, T.M.B.; Thim, G.P.; Trichês, E.D.S.; Prado, R.F.D.; Vasconcellos, L.M.R.D. β-TCP/S53P4 Scaffolds Obtained by Gel Casting: Synthesis, Properties, and Biomedical Applications. *Bioengineering* **2023**, *10*, 597. [CrossRef] [PubMed]
14. Akçay, H.; Tatar, B.; Kuru, K.; Ünal, N.; Şimşek, F.; Ulu, M.; Karaman, O. Comparison of Particulate, Block and Putty Forms of β-tricalcium Phosphate-Based Synthetic Bone Grafts on Rat Calvarium Model. *J. Maxillofac. Oral. Surg.* **2023**, *22*, 296–303. [CrossRef] [PubMed]
15. Akbari, S.; Saberi, E.A.; Fakour, S.R.; Heidari, Z. Immediate to short-term inflammatory response to biomaterial implanted in calvarium of mice. *Eur. J. Transl. Myol.* **2022**, *33*, 10785. [CrossRef] [PubMed]
16. Gupta, A.K.; Arora, K.S.; Aggarwal, P.; Kaur, K.; Mohapatra, S.; Pareek, S. Evaluation of biphasic hydroxapatite and β-tricalcium phosphate as a bone graft material in the treatment of periodontal vertical bony defects—A clinical and digital radiological measurement study. *Indian J. Dent. Res.* **2022**, *33*, 152–157. [PubMed]
17. Pinipe, J.; Mandalapu, N.B.; Manchala, S.R.; Mannem, S.; Gottumukkala, N.V.; Koneru, S. Comparative evaluation of clinical efficacy of β-tri calcium phosphate (Septodont-RTR)™ alone and in combination with platelet rich plasma for treatment of intrabony defects in chronic periodontitis. *J. Indian Soc. Periodontol.* **2014**, *18*, 346–351. [PubMed]
18. Brkovic, B.; Prasad, H.S.; Konandreas, G.; Milan, R.; Antunovic, D.; Sándor, G.K.; Rohrer, M.D. Simple preservation of a maxillary extraction socket using beta-tricalcium phosphate with type I collagen: Preliminary clinical and histomorphometric observations. *J. Can. Dent. Assoc.* **2008**, *74*, 523–528. [PubMed]
19. Hirota, M.; Matsui, Y.; Mizuki, N.; Kishi, T.; Watanuki, K.; Ozawa, T.; Fukui, T.; Shoji, S.; Adachi, M.; Monden, Y.; et al. Combination with allogenic bone reduces early absorption of beta-tricalcium phosphate (beta-TCP) and enhances the role as a bone regeneration scaffold. Experimental animal study in rat mandibular bone defects. *Dent. Mater. J.* **2009**, *28*, 153–161. [CrossRef]
20. Bernabé, P.F.; Melo, L.G.; Cintra, L.T.; Gomes-Filho, J.E.; Dezan, E., Jr.; Nagata, M.J. Bone healing in critical-size defects treated with either bone graft, membrane, or a combination of both materials: A histological and histometric study in rat tibiae. *Clin. Oral. Implant. Res.* **2012**, *23*, 384–388.
21. Schmitz, J.P.; Hollinger, J.O. The critical size defect as an experimental model for craniomandibulofacial nonunions. *Clin. Orthop. Relat. Res.* **1986**, *205*, 299–308. [CrossRef]
22. Xu, J.; Shen, J.; Sun, Y.; Wu, T.; Sun, Y.; Chai, Y.; Kang, Q.; Rui, B.; Li, G. In vivo prevascularization strategy enhances neovascularization of β-tricalcium phosphate scaffolds in bone regeneration. *J. Orthop. Transl.* **2022**, *37*, 143–151. [CrossRef] [PubMed]
23. Yoshino, Y.; Miyaji, H.; Nishida, E.; Kanemoto, Y.; Hamamoto, A.; Kato, A.; Sugaya, T.; Akasaka, T. Periodontal tissue regeneration by recombinant human collagen peptide granules applied with β-tricalcium phosphate fine particles. *J. Oral. Biosci.* **2023**, *65*, 62–71. [CrossRef] [PubMed]
24. Tian, Y.; Ma, H.; Yu, X.; Feng, B.; Yang, Z.; Zhang, W.; Wu, C. Biological response of 3D-printed β-tricalcium phosphate bioceramic scaffolds with the hollow tube structure. *Biomed. Mater.* **2023**, *18*, 034102. [CrossRef] [PubMed]

25. Luvizuto, E.R.; Queiroz, T.P.; Margonar, R.; Panzarini, S.R.; Hochuli-Vieira, E.; Okamoto, T.; Okamoto, R. Osteoconductive properties of β-tricalcium phosphate matrix, polylactic and polyglycolic acid gel, and calcium phosphate cement in bone defects. *J. Craniofac. Surg.* **2012**, *23*, e430–e433. [CrossRef] [PubMed]
26. Jeong, C.H.; Kim, J.; Kim, H.S.; Lim, S.Y.; Han, D.; Huser, A.J.; Lee, S.B.; Gim, Y.; Ji, J.H.; Kim, D.; et al. Acceleration of bone formation by octacalcium phosphate composite in a rat tibia critical-sized defect. *J. Orthop. Transl.* **2022**, *37*, 100–112. [CrossRef] [PubMed]
27. Li, J.; Li, J.; Yang, Y.; He, X.; Wei, X.; Tan, Q.; Wang, Y.; Xu, S.; Chang, S.; Liu, W. Biocompatibility and osteointegration capability of β-TCP manufactured by stereolithography 3D printing: In vitro study. *Open Life Sci.* **2023**, *18*, 20220530. [CrossRef] [PubMed]
28. Samavedi, S.; Whittington, A.R.; Goldstein, A.S. Calcium phosphate ceramics in bone tissue engineering: A review of properties and their influence on cell behavior. *Acta Biomater.* **2013**, *9*, 8037–8045. [CrossRef] [PubMed]
29. Cheng, L.; Shi, Y.; Ye, F.; Bu, H. Osteoinduction of calcium phosphate biomaterials in small animals. *Mater. Sci. Eng. C Mater. Biol. Appl.* **2013**, *33*, 1254–1260. [CrossRef] [PubMed]
30. Bueno, C.R.E.; Cintra, L.T.A.; Benetti, F.; Dal Fabbro, R.; Jacinto, R.C.; Dezan-Junior, E. Bioceramic Materials. In *Bioactive Materials in Dentistry: Remineralization and Biomineralization*; Benetti, F., Ed.; Nova Science Publishers, Inc.: New York, NY, USA, 2019; pp. 45–92.
31. Truedsson, A.; Wang, J.S.; Lindberg, P.; Gordh, M.; Sunzel, B.; Warfvinge, G. Bone substitute as an on-lay graft on rat tibia. *Clin. Oral. Implant. Res.* **2010**, *21*, 424–429. [CrossRef]
32. Ghanaati, S.; Barbeck, M.; Orth, C.; Willershausen, I.; Thimm, B.W.; Hoffmann, C.; Rasic, A.; Sader, R.A.; Unger, R.E.; Peters, F.; et al. Influence of β-tricalcium phosphate granule size and morphology on tissue reaction in vivo. *Acta Biomater.* **2010**, *6*, 4476–4487. [CrossRef] [PubMed]
33. Martinez, A.; Balboa, O.; Gasamans, I.; Otero-Cepeda, X.L.; Guitian, F. Deproteinated bovine bone vs. beta-tricalcium phosphate as bone graft substitutes: Histomorphometric longitudinal study in the rabbit cranial vault. *Clin. Oral. Implant. Res.* **2015**, *26*, 623–632. [CrossRef] [PubMed]
34. Benetti, F.; Bueno, C.R.E.; Reis-Prado, A.H.D.; Souza, M.T.; Goto, J.; Camargo, J.M.P.D.; Duarte, M.A.H.; Dezan-Júnior, E.; Zanotto, E.D.; Cintra, L.T.A. Biocompatibility, Biomineralization, and Maturation of Collagen by RTR®, Bioglass and DM Bone® Materials. *Braz. Dent. J.* **2020**, *31*, 477–484. [CrossRef] [PubMed]
35. Yamaguchi, M.; Shimizu, N.; Shibata, Y.; Abiko, Y. Effects of different magnitudes of tension-force on alkaline phosphatase activity in periodontal ligament cells. *J. Dent. Res.* **1996**, *75*, 889–894. [CrossRef] [PubMed]
36. Fathima, H. Osteostimulatory effect of bone grafts on fibroblast cultures. *J. Nat. Sci. Biol. Med.* **2015**, *6*, 291–294. [CrossRef]
37. Wancket, L.M. Animal Models for Evaluation of Bone Implants and Devices: Comparative Bone Structure and Common Model Uses. *Vet. Pathol.* **2015**, *52*, 842–850. [CrossRef]
38. Niederauer, G.G.; Niederauer, G.M.; Cullen, L.C., Jr.; Athanasiou, K.A.; Thomas, J.B.; Niederauer, M.Q. Correlation of cartilage stiffness to thickness and level of degeneration using a handheld indentation probe. *Ann. Biomed. Eng.* **2004**, *32*, 352–359. [CrossRef] [PubMed]
39. Cardoso, H.F. Epiphyseal union at the innominate and lower limb in a modern Portuguese skeletal sample, and age estimation in adolescent and young adult male and female skeletons. *Am. J. Phys. Anthropol.* **2008**, *135*, 161–170. [CrossRef] [PubMed]
40. Kunert-Keil, C.; Scholz, F.; Gedrange, T.; Gredes, T. Comparative study of biphasic calcium phosphate with beta-tricalcium phosphate in rat cranial defects--A molecular-biological and histological study. *Ann. Anat.* **2015**, *199*, 79–84. [CrossRef] [PubMed]
41. Borrasca, A.G.; Aranega, A.M.; Filho, O.M.; Timóteo, C.A. Bone repair of surgical defects filled with autogenous bone and covered with demineralized bone matrix membrane or polytetrafluoroethylene membrane in rats. *Int. J. Oral. Maxillofac. Implant.* **2015**, *30*, 442–449. [CrossRef] [PubMed]
42. Ribeiro, L.L.; Bosco, A.F.; Nagata, M.J.; de Melo, L.G. Influence of bioactive glass and/or acellular dermal matrix on bone healing of surgically created defects in rat tibiae: A histological and histometric study. *Int. J. Oral. Maxillofac. Implant.* **2008**, *23*, 811–817.
43. Mendes, S.M.; Fonseca, C.E.; Bassi, A.P.F.; Ponzoni, D. Carvalho PSP. Histologic and histomorphometric evaluation of heterogenous demineralized bone or compound bone with and without bone morphogenetic protein (bmp) in rat tíbia. *Rev. Odontológica Araçatuba* **2006**, *27*, 34–40.
44. Cunha, L.R.; Balducci-Roslindo, E.; Minarelli-Gaspar, A.M. Efeito do fosfato tricálcio na reparação de defeito ósseo em tíbias de ratos. *Rev. Odontol. UNESP* **2007**, *36*, 293–298.
45. Yuan, J.; Cui, L.; Zhang, W.J.; Liu, W.; Cao, Y. Repair of canine mandibular bone defects with bone marrow stromal cells and porous beta-tricalcium phosphate. *Biomaterials* **2007**, *28*, 1005–1013. [CrossRef]